The POD Dirichlet Boundary Control of the Navier-Stokes Equations: A Low-dimensional Approach to Optimal Control with High Smoothness

Ying Wang[1], Fredi Tröltzsch[2], and Günter Bärwolff[2]

[1] TU Braunschweig, Institute for computational modeling in civil engineering, D-38106 Braunschweig, Mühlenpfordtstraße 4-5, Germany
[2] TU Berlin, Institute of Mathematics, D-10623 Berlin, Str. d. 17. Juni 135, Germany

Summary. The proper orthogonal decomposition(POD) is an approach to capture a reduced order basis functions for a dynamical system. Utilizing the order reduction property of POD basis for minimizing computational cost to unsteady fluid flow control problem, we present a POD-based framework of the unsteady Dirichlet boundary control problem for Navier-Stokes equations. An extra basis function can be therefor constructed and appended into the general POD subspace, which as a key step enables the POD approach to the Dirichlet boundary control and results in the control problem merely in time scale. In the paper the excellent quality and flexibility of the POD approach to Dirichlet boundary flow control are confirmed numerically in several flow matching control examples.

Key words: Dirichlet boundary control, Galerkin POD method, reduced order models, Navier-Stokes equations

1 Introduction

Numerical flow simulation is computationally expensive for the purpose of unsteady fluid flow control. Recent development in computational methods for the control problems is therefore the design of model reduction to carry out the flow control problems with less effort. The proper orthogonal decomposition is one of the most widely applied methods for this purpose.

In the paper, we study the Dirichlet boundary flow control by using Galerkin POD, for which the fluid motion can be controlled by injection along a piece of boundary. The cost functional for flow matching is expressed as a measure of the distance between the controlled velocity and a given target flow. The control problem is subject to the unsteady Navier-Stokes equations

for viscous, incompressible fluid. This subject has been studied by many authors, e.g., [2–4, 7, 8].

The POD was first proposed by Lumley [11] in 1967, as a mathematical technique to extract a typical structure from turbulence flows. Numerous literature in the past two decades signifies the great progress in theoretical, numerical analysis and computational aspects especially for optimization, e.g. [1, 10, 13, 14, 18–20].

The Galerkin proper orthogonal decomposition provides possibility for deriving reduced order models of dynamical systems, which is in general described by PDEs. It is based on projecting the governing PDEs onto a proper subspace of snapshots ensemble, which is composed of the solutions for this dynamical system at pre-specified time distances or even experimental measurements. However, the snapshots are not suitable as the basis for the ensemble spanned by themselves due to the possible linear dependence. The global optimal orthogonal basis for the ensemble can be identified by solving an eigenvalue problem, and these basis will be denoted as POD basis. The number of these POD basis can be very small in comparison with the number of snapshots, which nevertheless carry the most dynamic energy of the system. The POD basis spanned subspace is the subspace onto which the dynamical system will be projected.

With Galerkin POD method we aim at not only reducing the computational cost of solving the nonlinear flow dynamics, but also achieving optimal Dirichlet boundary control for the Navier-Stokes equations. An access to the subject is firstly to make a new ansatz for the solution of the Navier-Stokes equations containing an extra basis function which is extracted from the spatial boundary behavior along the time, subsequently summarize the control action merely in a time dependent function. To guarantee its smoothness in the Dirichlet boundary condition, the explicit control parameter coupled in the control problem description would be its first time derivative. We apply Galerkin POD method to qualify this layout for the Dirichlet boundary control. This approach results in a new control problem in time scale, which facilitates computation during the numerical optimization.

The paper is organized as follows. In section 2, we define the Dirichlet boundary control problem subjects to the Navier-Stokes equations and quote the well-posedness of the state equations. The optimality system based on a Lagrangian technique including adjoint equation and variational inequality is derived in section 3. Section 4 is devoted briefly to theory of Galerkin POD, which associates the Dirichlet boundary control problem with the modified one into an optimal control problem in time scale. We illustrate the feature of the POD subspace, comparison full and reduced order simulations and provide numerical results of the optimization with Galerkin POD in section 5.

2 The Dirichlet Boundary Flow Control Problem

The incompressible fluid flow described by the Navier-Stokes equations in a $\Omega \subseteq \mathbb{R}^2$ throughout $[0, T]$ is characterized by the following quantities:

$$\mathbf{u}: \quad Q := \Omega \times [0, T] \to \mathbb{R}^2 \quad \text{velocity field,}$$
$$p: \quad Q := \Omega \times [0, T] \to \mathbb{R} \quad \text{pressure.}$$

The boundaries of the spatial domain Ω consist of the inflow boundary Γ_i, outflow boundary Γ_o and solid wall $\Gamma_s := \Gamma \backslash (\Gamma_i \cup \Gamma_o)$. A controllable design parameter will be set on the inflow boundary Γ_i. For the solid wall Γ_s and outflow Γ_o, we apply the nonslip boundary and open boundary condition, the

latter was detailed in [15].

We intend to find an optimal control z for the following Dirichlet boundary control problem

$$\min J(\mathbf{u}, z) = \frac{1}{2} \int_0^T \|\mathbf{u}(t, \cdot) - U_d\|_H^2 dt + \frac{\sigma_1}{2} \int_0^T z^2(t) dt$$

subject to

$$
\begin{aligned}
\mathbf{u}_t - \frac{1}{Re}\Delta\mathbf{u} + (\mathbf{u}\cdot\nabla)\mathbf{u} + \nabla p &= 0 && \text{in } Q \\
\nabla\cdot\mathbf{u} &= 0 && \text{in } Q \\
\mathbf{u}(\mathbf{x}, t) &= z(t)\mathbf{g}(\mathbf{x}) && \text{on } \Sigma_i := \Gamma_i \times [0, T] \\
p\nu - \frac{1}{Re}\frac{\partial\mathbf{u}}{\partial\nu} &= (0, 0) && \text{on } \Sigma_o := \Gamma_o \times [0, T] \\
\mathbf{u}(\mathbf{x}, t) &= (0, 0) && \text{on } \Sigma_s := \Gamma_s \times [0, T] \\
\mathbf{u}(\mathbf{x}, 0) &= \mathbf{u}_0(\mathbf{x}) && \text{in } \Omega
\end{aligned}
$$

in the set of admissible controls

$$\mathcal{U}_{ad} = \{z \in L^2(0, T) : z_a(t) \le z(t) \le z_b(t) \quad \text{a.e. on } (0, T)\}.$$

2.1 Preliminary results

First of all, we present the existence and uniqueness of weak solution for the inhomogeneous Navier-Stokes equations. Let H, V and V_0 be solenoidal spaces

$$H := \{\mathbf{v} \in L^2(\Omega)^2 : \nabla\cdot\mathbf{v} = 0\}, \quad V := \{\mathbf{v} \in H^1(\Omega)^2 : \nabla\cdot\mathbf{v} = 0\} \quad \text{and}$$
$$V_0 := \{\mathbf{v} \in H_0^1(\Omega)^2 : \nabla\cdot\mathbf{v} = 0\}.$$

The constraint $\nabla\cdot\mathbf{v} = 0$ is equivalent to $\langle\mathbf{v}, \nabla p\rangle = 0$ for all $p \in H^1(\Omega)$. By identifying H and its dual H', we obtain the well-defined Gelfand triple

$$V \hookrightarrow H = H' \hookrightarrow V',$$

each embedding being continuous and dense.

The inner product in V_0 is given by a symmetric bounded, coercive bilinear form $a : V_0 \times V_0 \to \mathbb{R}$:

$$a(\mathbf{u}, \mathbf{v}) = \langle\nabla\mathbf{u}, \nabla\mathbf{v}\rangle_{L^2(\Omega)^2} = \int_\Omega \sum_{i=1}^2 \nabla\mathbf{u}_i \cdot \nabla\mathbf{v}_i \, d\mathbf{x}. \tag{1}$$

Moreover, we introduce trilinear form $b : H^1(\Omega)^2 \times H^1(\Omega)^2 \times H^1(\Omega)^2 \to \mathbb{R}$ as the weak formulation of the Navier-Stokes nonlinearity $(\mathbf{u}\cdot\nabla)\mathbf{u}$ by

$$b(\mathbf{u}, \mathbf{v}, \mathbf{w}) = \langle(\mathbf{u}\cdot\nabla)\mathbf{v}, \mathbf{w}\rangle = \int_\Omega \sum_{i,j=1}^2 \mathbf{u}_i(D_i\mathbf{v}_j)\mathbf{w}_j \, d\mathbf{x}, \tag{2}$$

and b satisfies $b(\mathbf{u}, \mathbf{v}, \mathbf{w}) = -b(\mathbf{u}, \mathbf{w}, \mathbf{v})$ for all $\mathbf{u} \in V_0$ and $\mathbf{v}, \mathbf{w} \in H^1(\Omega)^2$.

To deal with the time derivative in the Navier-Stokes equations, we turn to the space of functions $\mathbf{u}$, whose time derivative $\mathbf{u}_t$ exists as abstract function in

$$W(0, T) := W^2(0, T; V_0) = \{\mathbf{u} \in L^2(0, T; V_0) : \mathbf{u}_t \in L^2(0, T; V_0')\}$$

endowed with norm

$$\|\mathbf{u}\|_{W(0,T)} = \|\mathbf{u}\|_{L^2(0,T;V_0)} + \|\mathbf{u}_t\|_{L^2(0,T;V_0')} .$$

$W(0,T)$ is Hilbert space and continuous embedded in $C([0,T], V_0)$, for the detail we refer to [17]. Since the state equation (1) due to boundary control must not pose homogeneous Dirichlet boundary all the time, the further space definition is therefore necessary to be initiated by following [8]

$$W^2(0,T;V) := \{\mathbf{u} \in L^2(0,T;V) : \mathbf{u}_t \in L^2(0,T;V_0')\},$$

endowed with norm

$$\|\mathbf{u}\|_{W^2(0,T;V)} = \|\mathbf{u}\|_{L^2(0,T;V)} + \|\mathbf{u}_t\|_{L^2(0,T;V_0')} .$$

To describe all solutions of the unsteady Navier-Stokes equations with the admissible inhomogeneous Dirichlet boundary conditions, we specify

$$W_{\Sigma_i} := \{g = \tau\hat{g} : \hat{g} \in W^2(0,T;V)\} \tag{3}$$

endowed with norm

$$\|g\|_{W_{\Sigma_i}} = \inf\{\|\hat{g}\|_{W^2(0,T;V)} : \tau\hat{g} = g, \quad \hat{g} \in W^2(0,T;V)\}. \tag{4}$$

Here $\tau : W^2(0,T;V) \to L^2(H^{1/2}(\Gamma_i)^2)$ is the trace operator given by

$$(\tau g)(t) = g(t,\cdot)\big|_{\Gamma_i} \quad \text{for almost every } t \in [0,T]. \tag{5}$$

Lemma 1. *For every* $\mathbf{u}_i = z(t)g(\mathbf{x}) \in W_{\Sigma_i}$, *there exists* $\tilde{\mathbf{u}} \in W^2(0,T;V)$ *which achieves the infimum in (4).*

For the proof of Lemma 1 and the detailed properties of the space W_{Σ_i}, we refer the reader to [8].

Theorem 1. *For every* $\mathbf{u}_i \in W_{\Sigma_i}$ *with* $\tilde{\mathbf{u}} \in W^2(0,T;V)$ *(see Lemma 1) and every divergence free* $\mathbf{u}_0 \in H$ *with* $\mathbf{u}_0 - \tilde{\mathbf{u}}(0) \in V_0$, *there exists a unique weak solution* $\mathbf{u} \in W^2(0,T;V)$ *for inhomogeneous Navier-Stokes equations, namely*

$$\langle\mathbf{u}_t, \mathbf{v}\rangle_{L^2(V_0'),L^2(V_0)} + \frac{1}{Re}\langle\nabla\mathbf{u}, \nabla\mathbf{v}\rangle + \langle(\mathbf{u}\cdot\nabla)\mathbf{u}, \mathbf{v}\rangle \quad = 0 \quad \text{for all } \mathbf{v} \in L^2(V_0),$$

$$\tau\mathbf{u} = \mathbf{u}_i \quad \text{in } W_{\Sigma_i},$$

$$\mathbf{u}(0,\cdot) = \mathbf{u}_0 \quad \text{in } H,$$

where $L^2(V_0)$ *denotes the* $L^2(0,T;V_0)$ *and* $L^2(V_0') = L^2(0,T;V_0')$.

For the existence and uniqueness of solution for the inhomogeneous Navier-Stokes equations and the corresponding proof, we refer to [8, Theorem 1.2]. Here we do not repeat the relevant context from [8] for the existence and uniqueness of optimal solution for the Dirichlet boundary control problem.

3 The Equivalently Modified Dirichlet Boundary Control Problem

Differing from the Dirichlet boundary control problem given above, we proceed equivalently a modified one such that the high smoothness of the design parameter z can be obtained. We can achieve this goal by restricting the time dependent function $z(t)$ on Σ_i of the Navier-Stokes flow (1) as follows

$$z(t) = \int_0^t v(s)ds + z_0 \,, \qquad (6)$$

which implies $z(t)$ to satisfy

$$\begin{cases} z'(t) = v(t) & \text{on } [0,T], \\ z(0) = z_0 \,. \end{cases} \qquad (7)$$

Modification of the Dirichlet boundary control problem is to permit $v(t)$ as the design parameter instead of $z(t)$. It seems to obtain a more complicated control problem, which consists of one cost functional and two state equations, namely

$$\min J(\mathbf{u}, z, v) = \frac{1}{2} \int_0^T \|\mathbf{u}(t,\cdot) - U_d\|_H^2 dt + \frac{\sigma_1}{2} \int_0^T z^2(t)dt + \frac{\sigma}{2} \int_0^T v^2(t)dt \qquad (8)$$

subject to

$$\mathbf{u}_t - \frac{1}{Re}\Delta\mathbf{u} + (\mathbf{u}\cdot\nabla)\mathbf{u} + \nabla p = 0 \quad \text{in } Q,$$
$$\nabla\cdot\mathbf{u} = 0 \quad \text{in } Q,$$
$$\mathbf{u}(\mathbf{x},t) = z(t)\mathbf{g}(\mathbf{x}) \quad \text{on } \Sigma_i,$$
$$p\nu - \frac{1}{Re}\frac{\partial\mathbf{u}}{\partial\nu} = (0,0) \quad \text{on } \Sigma_o,$$
$$\mathbf{u}(\mathbf{x},t) = (0,0) \quad \text{on } \Sigma_s,$$
$$\mathbf{u}(\mathbf{x},0) = \mathbf{u}_0(\mathbf{x}) \quad \text{in } \Omega,$$

$$z'(t) = v(t) \quad \text{on } [0,T],$$
$$z(0) = z_0 \,.$$

With an assumption $\sigma_1 = 0$ throughout the paper, the set of admissible controls should be altered as

$$\mathcal{U}_{ad} = \{v \in L^2(0,T) : v_a(t) \le v(t) \le v_b(t) \quad \text{a.e. on } (0,T)\}\,.$$

We devote to derive the necessary optimality condition with help of the formal Lagrangian Multiplier. The Lagrangian technique is known to deliver in general the correct first order optimality conditions. For that a mathematically rigorous proof is not presented.

Define the Lagrangian function

$$\mathcal{L}(\mathbf{u}, p, z, v, \{\eta_i\}_{i=1}^3, \pi, \zeta)$$
$$:= J(\mathbf{u}, v) - \iint_Q \left[\mathbf{u}_t - \frac{1}{Re}\Delta\mathbf{u} + (\mathbf{u}\cdot\nabla)\mathbf{u} + \nabla p\right]\cdot\eta_1\,d\mathbf{x}\,dt$$

$$- \iint_Q \pi\left[-\nabla\cdot\mathbf{u}\right]d\mathbf{x}\,dt - \iint_{\Sigma_i}\left[z(t)\mathbf{g}(\mathbf{x}) - \mathbf{u}\right]\cdot\eta_2\,ds(\mathbf{x})\,dt \qquad (9)$$

$$- \iint_{\Sigma_o}\left[\frac{1}{Re}\frac{\partial\mathbf{u}}{\partial\nu} - p\nu\right]\cdot\eta_3\,ds(\mathbf{x})\,dt - \int_\Omega\left[\mathbf{u}(0,\mathbf{x}) - \mathbf{u}_0(\mathbf{x})\right]\cdot\eta_1(0,\mathbf{x})d\mathbf{x}$$

$$- \int_0^T\left[z'(t) - v(t)\right]\zeta(t)dt - \left(z(0) - z_0\right)\zeta(0)$$

with the Lagrangian multipliers $\{\eta_i\}_{i=1}^3$, π and ζ respectively to the three states $\mathbf{u}, p$ and z. According to the Lagrangian principle, we expect the following equations and variation inequality to be valid at the local minimal denoted by $(\mathbf{u}^*, p^*, z^*, v^*, \{\eta_i\}_{i=1}^3, \pi, \zeta)$

$$\begin{cases} D_{\mathbf{u}}\mathcal{L}(\mathbf{u}^*, p^*, z^*, v^*, \{\eta_i\}_{i=1}^3, \pi, \zeta) \cdot \mathbf{u} = 0, & \forall\, \mathbf{u}, \\ D_p\mathcal{L}(\mathbf{u}^*, p^*, z^*, v^*, \{\eta_i\}_{i=1}^3, \pi, \zeta)\, p = 0, & \forall\, p, \\ D_z\mathcal{L}(\mathbf{u}^*, p^*, z^*, v^*, \{\eta_i\}_{i=1}^3, \pi, \zeta)\, z = 0, & \forall\, z, \\ D_v\mathcal{L}(\mathbf{u}^*, p^*, z^*, v^*, \{\eta_i\}_{i=1}^3, \pi, \zeta)\, (v^* - v) \geq 0, & \forall\, v. \end{cases} \quad (10)$$

A similar calculation can be found in [21]. Here we give the adjoint equation which is derived by summarizing $\eta\big|_{\Sigma_o} = \eta_3$ and otherwise $\eta = \eta_1$

$$-\eta_t - \frac{1}{Re}\Delta\eta + (\nabla\mathbf{u}^*)\eta - (u^* \cdot \nabla)\eta + \nabla\pi = \mathbf{u}^* - U_d \ \text{ in } Q \qquad (11)$$

$$\nabla \cdot \eta = 0 \ \text{ in } Q \qquad (12)$$

$$\pi\nu - \frac{1}{Re}\frac{\partial\eta}{\partial\nu} = 0 \ \text{ on } \Sigma_o \qquad (13)$$

$$\eta = 0 \ \text{ on } \Sigma\backslash\Sigma_o \qquad (14)$$

$$\eta(\cdot, T) = 0 \ \text{ in } \Omega \qquad (15)$$

$$\eta_2 = \frac{1}{Re}\frac{\partial\eta}{\partial\nu} - \pi\nu \ \text{ on } \Sigma_i \qquad (16)$$

$$\zeta'(t) = \mathbf{g}(\mathbf{x}) \cdot \eta_2 \ \text{ on } [0, T] \qquad (17)$$

$$\zeta(T) = 0 \qquad (18)$$

and the variation inequality

$$\int_0^T \big[\sigma v(t) - \zeta(t)\big](v^*(t) - v(t))dt \geq 0, \quad \forall v \in \mathcal{U}_{ad}\,.$$

It is quite expensive to solve such an optimization system iteratively. For each iteration one must deal with the parabolic nonlinear PDE (1), the parabolic linearized PDE (11-15) and the ODE (17-18). Insisting on the optimal solution for this modified control problem without so much computational cost, we could however still employ an order reduction approach, e.g., Galerkin POD method.

4 The Proper Orthogonal Decomposition

Briefly a general aspect of the POD subspace is introduced, which contains understanding, finding and using the POD basis functions. The principle behind the proper orthogonal decomposition is to capture the POD basis as an orthogonal basis system in a certain finite space by minimizing a least-square error formula. To find them numerically, one may utilize the singular value decomposition theorem to facilitate the computation. At end of this section we introduce the way to validate the modified Dirichlet boundary control problem merely in time scale.

4.1 The discrete POD

Given $n \in \mathbb{N}$ and $0 = t_1 \leq t_2 \leq, ..., \leq t_n \leq T$, for convenience suppose equivalent time difference. Then the solution of the Navier-Stokes equation $\{\mathbf{u}(t_j)\}_{j=1}^n$, which are also called snapshots, can be either obtained numerically or experimentally with reference to this time discretization $\{t_j\}_{j=1}^n$. Let us denote the snapshots ensemble by $\mathcal{V}_n = span\{\mathbf{u}(t_1), ..., \mathbf{u}(t_n)\} \subset V$, and $1 \leq \dim \mathcal{V}_n \leq n$, i.e., at least one of the snapshots is nonzero.

Let $\{\phi_k\}_{k=1}^n$ denote the orthonormal basis for $\mathcal{V}_n$. Then each member of the ensemble can be expressed as follows

$$\mathbf{u}(t_j) = \sum_{k=1}^n \langle \mathbf{u}(t_j), \phi_k \rangle_V \phi_k \quad \text{for } j = 1, ..., n\,.$$

It is expected that a few of the orthonormal basis $\{\phi_k\}_{k=1}^n$ can represent a typical structure of the ensemble. One way to solve the problem is with M orthonormal basis of $\{\phi_k\}_{k=1}^n$ to yield the maximal projection of the snapshots, i.e., $\{\phi_k\}_{k=1}^n$ spanned subspace. In mathematical language, the task is to find $M \leq n$, such that the orthonormal system $\{\phi_k\}_{k=1}^M$ of $\mathcal{V}_n$ minimizes the following least-square error:

$$\begin{cases} \min_{\{\phi_k\}_{k=1}^M} \sum_{j=1}^n \alpha_j \left\| \mathbf{u}(t_j) - \sum_{k=1}^M \langle \mathbf{u}(t_j), \phi_k \rangle \phi_k \right\|_V^2\,, \\[2mm] \text{subject to} \quad \langle \phi_i, \phi_j \rangle_V = \delta_{ij}, \quad 1 \leq i, j \leq M\,, \end{cases} \quad (19)$$

where $\{\alpha_k\}_{k=1}^n$ are positive weights chosen for the purpose of integration, e.g.,

$$\alpha_1 = \frac{\Delta t}{2}, \quad \alpha_j = \Delta t, \quad j = 2, ..., n-1, \quad \alpha_n = \frac{\Delta t}{2}\,.$$

Then we define a linear mapping $\mathcal{Y}_n \in L(\mathbb{R}^n, \mathcal{V}_n)$ with $\mathcal{Y}_n(e_k) = \mathbf{u}_k = \mathbf{u}(t_k)$, where $\{e_k\}_{k=1}^n$ denote the canonical basis in $\mathbb{R}^n$. For all $u \in \mathbb{R}^n$

$$\mathcal{Y}_n(u) = \sum_{j=1}^n \alpha_j \langle u, e_j \rangle_{\mathbb{R}^n} \mathbf{u}_j \quad (20)$$

where the inner scalar product in $\mathbb{R}^n$ is defined as

$$\langle v, w \rangle_{\mathbb{R}^n} = \sum_{k=1}^n \alpha_k v_k w_k\,.$$

Assume that $\mathcal{Y}_n^* : \mathcal{V}_n \to \mathbb{R}^n$ is the adjoint of $\mathcal{Y}_n$, then it follows for all $\phi \in \mathcal{V}_n$

$$\mathcal{Y}_n^* \phi = \left[\langle \mathbf{u}_1, \phi \rangle_V \cdots \langle \mathbf{u}_n, \phi \rangle_V \right]^T\,. \quad (21)$$

Define $\mathcal{R}_n := \mathcal{Y}_n \mathcal{Y}_n^* \in L(\mathcal{V}_n)$ and $\mathcal{K}_n := \mathcal{Y}_n^* \mathcal{Y}_n \in L(\mathbb{R}^n)$. Summarizing (20) for $\mathcal{Y}_n$ and (21) for $\mathcal{Y}_n^*$ yields

$$\mathcal{R}_n = \sum_{k=1}^n \alpha_k \langle \mathbf{u}_k, \cdot \rangle_V \mathbf{u}_k \quad (22)$$

$$\mathcal{K}_n = \left[\langle \mathbf{u}_1, \mathcal{Y}_n(\cdot) \rangle_V \cdots \langle \mathbf{u}_n, \mathcal{Y}_n(\cdot) \rangle_V \right]^T \quad (23)$$

where

$$\langle \mathbf{u}_k, \mathcal{Y}_n(\cdot)\rangle_V = \langle \begin{bmatrix} \langle \mathbf{u}_k, \mathbf{u}_1\rangle \\ \vdots \\ \langle \mathbf{u}_k, \mathbf{u}_n\rangle \end{bmatrix}, \cdot\rangle_{\mathbb{R}^n}.$$

Using a Lagrangian framework, the first order optimality condition for the least-square problem (19) is

$$\mathcal{R}_n \phi_i = \lambda_i \phi_i \quad \lambda_1 \geq \lambda_2 \geq \cdots \geq \lambda_n. \tag{24}$$

For a fuller treatment we refer the reader to [20]. By solving (24) we can capture the orthonormal basis $\{\phi_k\}_{k=1}^n$ that satisfies the first order optimality condition and is thus the local minimum for the least-square problem (19). However, by following [20] it can be proved that there is no orthogonal system with M basis in the snapshots ensemble which solves the least square problem better than the POD basis does and $\{\phi_k\}_{k=1}^M$ is thus global optimum with respect to a fixed M. By choosing M, the least-square error formula (19) can be evaluated as in the following theorem.

Theorem 2. *Let $\lambda_1 \geq \lambda_2 \geq \cdots \geq \lambda_n \geq 0$ denote the non-negative eigenvalues of $\mathcal{R}_n$ with the associated orthonormal eigenvectors $\{\phi_k\}_{k=1}^n$ in $\mathcal{V}_n$. Let $M \ll n$, then $\{\phi_k\}_{k=1}^M$ is orthonormal with rank M, and the least-square error formula (19) satisfies:*

$$\sum_{j=1}^n \alpha_j \|\mathbf{u}(t_j) - \sum_{k=1}^M \langle \mathbf{u}(t_j), \phi_k\rangle \phi_k\|_V^2 = \sum_{j=M+1}^n \lambda_j.$$

The proof is straightforward by utilizing the definitions of $\mathcal{R}_n$ and its property (24). In the following we give an example of the snapshots ensemble to examine the above mentioned properties of the operators $\mathcal{R}_n$ and $\mathcal{K}_n$.

Example 1. Let $n \in \mathbb{N}$ and $n < N$, where N is the number of spatial grids. The snapshots ensemble is

$$\mathcal{V}_n = span\{\mathbf{u}(t_1), ..., \mathbf{u}(t_n)\}.$$

The operators $\mathcal{R}_n$ and $\mathcal{K}_n$ are obtained by the definitions (22) and (23)

$$\mathcal{R}_n \phi = \sum_{k=1}^n \alpha_k \langle \mathbf{u}_k, \phi\rangle_V \mathbf{u}_k = \underbrace{\sum_{k=1}^n \alpha_k \mathbf{u}_k \mathbf{u}_k^T}_{:=R} \phi$$

$$\mathcal{K}_n u = \underbrace{\begin{pmatrix} \langle \mathbf{u}_1, \mathbf{u}_1\rangle & \cdots & \langle \mathbf{u}_1, \mathbf{u}_n\rangle \\ \vdots & \ddots & \vdots \\ \langle \mathbf{u}_n, \mathbf{u}_1\rangle & \cdots & \langle \mathbf{u}_n, \mathbf{u}_n\rangle \end{pmatrix}}_{:=K} u$$

One captures the POD basis system $\{\phi_k\}_{k=1}^n$ to minimize the least-square error formula (19) by solving (24), which is for this example equivalent to solve eigenvalue problem of the new defined R, namely

$$R\phi_i = \lambda_i \phi_i \quad \lambda_1 \geq \lambda_2 \geq \cdots \geq \lambda_n > 0, \ \lambda_{n+1} = \cdots = \lambda_N = 0.$$

Note that this by n snapshots generated $N \times N$ matrix R has n nonzero eigenvalues and N orthonormal eigenvectors $\{\phi_i\}_{i=1}^N$. For $M \ll n < N$, the M POD basis system $\{\phi_k\}_{k=1}^M$ can minimize the least-square error (19), which can be also evaluated according to Theorem 2.

Actually we would rather possibly solve eigenvalue problem for the matrix K with dimension n than for R with N, since R possesses only n non-zero eigenvalues in total and the number of time distances n is usually much smaller than the number of spatial grids N. By the theorem of singular value decomposition, the eigenvector of R can be also captured implicitly, i.e., with aid of the eigenvector of K and a linear mapping from $L(\mathbb{R}^n, \mathcal{V}_n)$. For that we find firstly an orthonormal basis $\{u_k\}_{k=1}^n$ in $\mathbb{R}^n$ such that for $k = 1, ..., n$

$$\mathcal{K}_n(u_k) = \lambda_k u_k \,.$$

The solution for the least-square problem (19) should be an orthonormal basis $\{\phi_k\}_{k=1}^M$ in $\mathcal{V}_n$. It is not difficult to utilize the linear mapping $\mathcal{Y}_n$ such that

$$\mathcal{Y}_n(u_k) = \sqrt{\lambda_k}\phi_k \quad \text{i.e., } \phi_k = \frac{1}{\sqrt{\lambda_k}}\mathcal{Y}_n(u_k) \tag{25}$$

for a fixed M and $k = 1, ..., M$.

For an exactly mathematical discussion of the continuous POD, which is essential for error estimates of Galerkin POD approximation, we refer to [10] and [18].

4.2 Construction of the POD basis functions

To capture the POD basis with the given snapshots, we discuss the practical algorithm based on the finite-dimensional POD. It is comparable to the snapshots method, which has been used by Ravindran in [13]. Note that from now on the POD basis will be written as $\{\boldsymbol{\Phi}_i\}_{i=1}^n$ and $\{\boldsymbol{\Phi}_i\}_{i=1}^M$ in order to emphasize POD basis function as vector field.

We begin by making an ansatz for the solution of the Navier-Stokes equation

$$\mathbf{u}(\mathbf{x}, t) = \mathbf{u}_m(\mathbf{x}) + \sum_{i=1}^M \beta_i(t)\boldsymbol{\Phi}_i(\mathbf{x}) + z(t)\mathbf{u}_z(\mathbf{x}), \tag{26}$$

where

$$\mathbf{u}_m = \frac{1}{n}\sum_{j=1}^n \mathbf{u}(\mathbf{x}, t_j) \,, \tag{27}$$

$$\mathbf{v}(\mathbf{x}, t) = \sum_{i=1}^M \beta_i(t)\boldsymbol{\Phi}_i(\mathbf{x}) \,. \tag{28}$$

It is noticed the steady flow $\mathbf{u}_z(\mathbf{x})$ remains unspecified. In view of qualifying the POD models for Dirichlet boundary fluid flow control, $z(t)\mathbf{u}_z(\mathbf{x})$ in the ansatz (26) is designed such that all spatial behaviors in the time interval $[0, T]$ are extracted into the steady flow $\mathbf{u}_z(\mathbf{x})$ and the scalar $z(t)$ is then assigned as time dependent control for accommodating $z(t)\mathbf{u}_z(\mathbf{x})$ to the Navier-Stokes solution with certain specified Dirichlet boundary condition. Therefore, in such a way the time dependent boundary control $z(t)$ is separated from the unsteady solution of the Navier-Stokes equations.

According to the definition (3) of W_{Σ_i} and Lemma 1, for every on Σ_i well-defined Dirichlet boundary $\mathbf{u}_i \in W_{\Sigma_i}$ there exist at least one solution $\tilde{\mathbf{u}} \in W^2(0, T; V)$ for the Navier-Stokes system (1), which satisfies the inflow Dirichlet boundary condition $\mathbf{u}_i$ on Σ_i, i.e.,

$$\tilde{\mathbf{u}}(\mathbf{x}, t)\big|_{\Sigma_i} = \mathbf{u}_i(\mathbf{x}, t) = z(t)\mathbf{g}(\mathbf{x}) \,.$$

Let us make the next important assumption

$$\tilde{\mathbf{u}}(\mathbf{x}, t) = z(t)\mathbf{u}_z(\mathbf{x}) \quad \text{in } Q.$$

Obviously if one captures a steady flow $\mathbf{u_g} \in V$ which satisfies the pre-specified inflow Dirilchlet boundary $\mathbf{g}(\mathbf{x})$, then equality holds in (29)

$$\mathbf{u}_z = \mathbf{u_g}, \tag{29}$$

where $\mathbf{g}(\mathbf{x})$ is defined in $L^2(H^{1/2}(\Gamma_i)^2)$ according to the definition (5) of trace operator τ. In the following we give another construction of $\mathbf{u}_z$, and assume the time dependent function $z(t)$ is given as a linear profile.

Example 2. Let

$$z(t) = z_s t + z_0, \quad t \in [0, T] \text{ and } z_s, z_0 \in \mathbb{R}. \tag{30}$$

The inflow boundary condition of the Navier-Stokes equations is defined for instance

$$z(t)\mathbf{g}(\mathbf{x}) = z(t) \begin{pmatrix} \sin(\frac{y-y_0}{y_1-y_0}\pi) \\ 0 \end{pmatrix} \quad \text{on } \Sigma_i,$$

where y_0 and y_1 are the inflow bounds in y-axis. The other settings for the Navier-Stokes equations remain unchanged as in the Dirichlet boundary control problem. For this system one can also construct the steady flow solution $\mathbf{u}_z$ by

$$\mathbf{u}_z(\mathbf{x}) = \frac{\mathbf{u}_{z_1}(\mathbf{x}) - \mathbf{u}_{z_0}(\mathbf{x})}{z_1 - z_0}, \tag{31}$$

where $z_1 = z_s T + z_0$ and z_0 is given as above. Note that $\mathbf{u}_{z_1}$ is the solution of the steady Navier-Stokes equation regarding the inflow boundary condition $z_1\mathbf{g}(\mathbf{x})$ on Γ_i and $\mathbf{u}_{z_0}$ is the ones with $z_0\mathbf{g}(\mathbf{x})$ on Γ_i as the inflow boundary condition.

It is also known that $\mathbf{u}_{z_1}$ has the same inflow boundary condition $z_1\mathbf{g}(\mathbf{x})$ on Γ_i as the steady flow $z_1\mathbf{u_g}$, where $\mathbf{u_g}$ is the steady flow regarding the inflow boundary condition $\mathbf{g}(\mathbf{x})$ on Γ_i. It is allowed to substitute the steady flow $\mathbf{u}_{z_1}$ with the steady flow $z_1\mathbf{u_g}$ and $\mathbf{u}_{z_0}$ with $z_0\mathbf{u_g}$ in (31), since both compatible pairs $(\mathbf{u}_{z_1}, z_1\mathbf{u_g})$ and $(\mathbf{u}_{z_0}, z_0\mathbf{u_g})$ have the same inflow boundary conditions on Γ_i respectively. Then one yields

$$\mathbf{u}_z(\mathbf{x}) = \frac{\mathbf{u}_{z_1}(\mathbf{x}) - \mathbf{u}_{z_0}(\mathbf{x})}{z_1 - z_0} = \frac{z_1\mathbf{u_g}(\mathbf{x}) - z_0\mathbf{u_g}(\mathbf{x})}{z_1 - z_0} = \mathbf{u_g}(\mathbf{x}),$$

which shows no conflict to (29).

Another advantage of using the above construction (31) lies in the fact that the graph of $z(t)$ for $t \in (0, T)$ can be skipped without breaking (29) and thus $z(t)$ must not constrained to be a linear function for $t \in (0, T)$. We will fix up a suitable numerical example to confirm the independence between $z(t)$ for $t \in (0, T)$ or for $t \in [t_0, t_1] \subset (0, T)$ and $\mathbf{u}_z$ in Ω, although they are expected by multiplying with each other to match the Dirichlet boundary condition $z(t)\mathbf{g}(\mathbf{x})$ on Σ_i.

Definition 1. *Let us define a modified ensemble set*

$$\mathcal{V}_0 = span\{\mathbf{v}_i\}_{i=1}^n,$$

where $\mathbf{v}_i$ is vector field

$$\mathbf{v}(\mathbf{x}, t) = \mathbf{u}(\mathbf{x}, t) - \mathbf{u}_m(\mathbf{x}) - z(t)\mathbf{u}_z(\mathbf{x}) \quad \text{defined at } t = t_i.$$

For the numerical algorithm one assumes that every POD basis $\mathbf{\Phi}$ has the form

$$\mathbf{\Phi}_i = \sum_{j=1}^{n} w_j^{(i)} \mathbf{v}_j \tag{32}$$

in terms of $\{\mathbf{v}_j\}_{j=1}^n$, where $w^{(i)}$ is to be determined such that $\mathbf{\Phi}$ minimizes the least square formula (19). By (20) and (25) in the finite-dimensional case, the eigenfunctions $\{\mathbf{\Phi}_i\}_{i=1}^n$ of $\mathcal{R}_n$ have the form

$$\mathbf{\Phi}_i = \frac{1}{\sqrt{\lambda_i}} \mathcal{Y}_n(u^{(i)}) = \frac{1}{\sqrt{\lambda_i}} \sum_{j=1}^{n} u_j^{(i)} \mathbf{v}_j , \tag{33}$$

where $u_j^{(i)}$ is the j-th component of the i-th eigenvector of $\mathcal{K}_n$. To coincide (32) with (33), we let

$$w_k^{(i)} = \frac{1}{\sqrt{\lambda_i}} u_k^{(i)}, \quad \text{for } k = 1, ..., n.$$

To determine the orthonormal basis $\{u_k\}_{k=1}^n$ for $\mathcal{K}_n$, one can solve the following eigenvalue problem,

$$\underbrace{\frac{1}{n} \mathcal{K}_n}_{C} u^{(i)} = \underbrace{\frac{\lambda_i}{n}}_{\Lambda_i} u^{(i)}$$

$$Cu^{(i)} = \Lambda_i u^{(i)} \quad i = 1, ..., n, \tag{34}$$

where C is the correlation matrix according to the $\mathcal{K}_n$'s definition (23) and Example 1 with components

$$\left[C\right]_{ij} = \frac{1}{n} \langle \mathbf{v}_i, \mathbf{v}_j \rangle_V, \quad \text{for } i, j = 1, ..., n.$$

It follows from the fact that C is a positive semi-definite symmetric matrix, which has a complete set of orthogonal eigenvectors $\{u^{(i)}\}_{i=1}^n$ along with a set of non-negative eigenvalues $\{\lambda_i\}_{i=1}^n$.

By Theorem 2 it is known that the least-square error can be evaluated as the sum of eigenvalues, i.e., $\sum_{i=M+1}^{n} \lambda_i$. It should be thus as small as possible. From that one can specify an energy level $0 < e < 1$ to be captured, and then seek $M \ll n$ such that

$$\frac{\sum_{i=1}^{M} \lambda_i}{\sum_{i=1}^{n} \lambda_i} > e \quad \text{and} \quad 0 \le \frac{\sum_{i=M+1}^{n} \lambda_i}{\sum_{i=1}^{n} \lambda_i} < 1 - e$$

Obviously $e = 1$ implies the full order models. We choose e to be close to 1 in the numerical computation such that the expected energy level e can be reached with M. The Algorithm 1 for construction of POD basis is given on page 12.

Utilizing the Galerkin projection of the Navier-Stokes equations onto the modified ensemble $\mathcal{V}_0$ (see Definition 1) yields a nonlinear ODE, which will be summarized in the following.

Lemma 2. *Let $\mathcal{V}_n$ denote the snapshots ensemble, all snapshots of which are determined by solving the Navier-Stokes equations (1) in a time interval $[0, T]$*

with the pre-specified inflow boundary condition. $\mathcal{V}_0$ is the modified ensemble defined in Definition 1. The POD basis $\{\boldsymbol{\Phi}_i\}_{i=1}^M$ spans the POD subspace $\mathcal{V}_{pod} \subset \mathcal{V}_0$. Then the POD reduced order models for the Navier-Stokes equations (1) is obtained for all $t \in (0, T]$

$$\dot{\mathbf{X}}(t) = \begin{pmatrix} 1' \\ \beta'(t) \\ z'(t) \end{pmatrix} = \begin{pmatrix} 0 \\ -\frac{1}{Re} A \, \mathbf{X}(t) - K(\mathbf{X}(t)) \\ 0 \end{pmatrix} + v(t) \begin{pmatrix} 0 \\ \tilde{B} \\ 1 \end{pmatrix} \qquad (35)$$

$$\mathbf{X}(0) = \begin{pmatrix} 1 & \beta(0) & z_0 \end{pmatrix}^T$$

where for $i = 1, ..., M$ and $j = 0, ..., M + 1$

$$\mathbf{F}(\mathbf{X}) = \begin{pmatrix} 0 \\ -\frac{1}{Re} A \, \mathbf{X}(t) - K(\mathbf{X}(t)) \\ 0 \end{pmatrix},$$

$$\left[A \right]_{i,j} = \langle \nabla \boldsymbol{\Phi}_i, \nabla \boldsymbol{\Phi}_j \rangle_{L^2(\Omega)^2},$$

$$K_i(\mathbf{X}(t)) = \mathbf{X}(t)^T P_i \mathbf{X}(t), \quad \left[P_i \right]_{k,l} = \langle (\boldsymbol{\Phi}_k \cdot \nabla) \boldsymbol{\Phi}_l, \boldsymbol{\Phi}_i \rangle_{L^2(\Omega)^2},$$

$$B = \begin{pmatrix} 0 \\ \tilde{B} \\ 1 \end{pmatrix}, \quad \left[\tilde{B} \right]_i = -\langle \boldsymbol{\Phi}_{M+1}, \boldsymbol{\Phi}_i \rangle_{L^2(\Omega)^2},$$

$$\left[\beta_0 \right]_i = \langle \mathbf{u}_0 - \mathbf{u}_m - z_0 \, \mathbf{u}_z, \boldsymbol{\Phi}_i \rangle_{L^2(\Omega)^2}$$

and $z'(t) = v(t)$ with $z(0) = z_0$, where $z(t)$ is the time dependent term of the inflow boundary condition for the Navier-Stokes equations (1).

The explicit proof we rely on [21]. In fact, the POD reduced order models consist of the POD weak solution of the Navier-Stokes equations, namely

---

Algorithm 1: Construction of POD basis

begin

- Define for $i = 1, ..., n$

$$\mathbf{v}_i(\mathbf{x}) = \mathbf{v}(\mathbf{x}, t_i) = \mathbf{u}(\mathbf{x}, t_i) - \mathbf{u}_m(\mathbf{x}) - z(t_i)\mathbf{u}_z(\mathbf{x}),$$

  where $\mathbf{u}_m(\mathbf{x})$ is defined as (27) and $\mathbf{u}_z(\mathbf{x})$ constructed as (31).
- Compute the symmetric correlative matrix C. Its entries are given

$$\left[C \right]_{i,j} = \frac{1}{n} \int\limits_\Omega \mathbf{v}_i(\mathbf{x}) \mathbf{v}_j(\mathbf{x}) \, d\mathbf{x}, \quad i, j = 1, ..., n.$$

- Solve the eigenvalue problem $CU = \Lambda U$.
- Prescribe an energy level e in percentage and find minimal $M \ll n$, such that

$$\frac{\sum\limits_{i=1}^M \lambda_i}{\sum\limits_{i=1}^n \lambda_i} > e,$$

  where $\lambda_i = n\Lambda_i$ and $\lambda_1 \geq ... \geq \lambda_M \geq \lambda_{M+1} \geq ... \geq \lambda_n \geq 0$.
- Obtain the POD basis with the expression

$$\boldsymbol{\Phi}_i = \frac{1}{\sqrt{\lambda_i}} \sum_{j=1}^n u_j^{(i)} \mathbf{v}_j, \quad i = 1, ..., M.$$

end

$$\beta'(t) = -\frac{1}{Re}A\mathbf{X}(t) - K(\mathbf{X}(t)) + z'(t)\tilde{B},$$

which is derivable by restricting the Navier-Stokes equation's POD ansatz (26) to the POD subspace $\mathcal{V}_{pod}$ with $L^2(\Omega^2)$ scalar product. It is not complete as a solvable differential equation, since there are $M + 1$ unknowns but only M equations. Therefore the POD weak solution is extended as in (35) by utilizing the second state equation of the modified Dirichlet boundary control problem

$$z'(t) = v(t) \quad \text{with} \quad z(0) = z_0.$$

For generating the snapshots we must pre-specify a Dirichlet boundary condition on Σ_i for the Navier-Stokes equations, which is included by the time dependent function $z(t)$ on $[0, T]$. Once $z(t)$ is specified, then $z'(t)$, i.e., $v(t)$ is also fixed. While solving the POD reduced order models (35), we have thus known which function as $v(t)$ on $[0, T]$ should be taken for the POD basis set.

The numerical recast of fluid flow is completed by solving the nonlinear ODE system (35) for $\mathbf{X}(t)$ and subsequently applying the POD ansatz (26) with $\mathbf{X}(t)$ and POD basis.

4.3 The POD Boundary Flow Control

It is convenient now to search a suboptimal triple $\{v(t), \mathbf{u}(\mathbf{x}, t), z(t)\}$ in the admissible set, the snapshots ensemble and $L^2([0, T])$ respectively, since both state equations of the modified Dirichlet boundary control problem can be substituted with the POD reduced order models (35). To find equivalently a optimal pair $(v(t), \mathbf{X}(t))$, we also need to revise the cost functional $J(\mathbf{u}, z, v)$ by projecting it onto the snapshots ensemble.

The new cost functional J should be with respect to a control parameter v and its associated state $\mathbf{X}$ by assuming $\sigma_1 = 0$ in (8). Except for substituting $\mathbf{u}(\cdot, t)$ in the cost functional (8) by the POD ansatz (26), $\mathbf{X}_d$ must be captured for a given expected flow pattern in the POD subspace. Let U_d the target flow, then induces

$$U_d(\mathbf{x}) = \mathbf{\Phi}_0(\mathbf{x}) + \sum_{i=1}^{M} \underbrace{\langle U_d(\mathbf{x}) - \mathbf{\Phi}_0(\mathbf{x}) - C_d\mathbf{\Phi}_{M+1}(\mathbf{x}), \mathbf{\Phi}_i(\mathbf{x})\rangle}_{:=\beta_{d,i}} \mathbf{\Phi}_i(\mathbf{x})$$
$$+ C_d\mathbf{\Phi}_{M+1}(\mathbf{x}), \tag{36}$$

where $\{\beta_{d,i}\}_{i=1}^{M}$ and C_d are summarized in a vector as

$$\mathbf{X}_d := [1, \quad \beta_{d,1}, \quad ... \quad, \quad \beta_{d,M}, \quad C_d]^T.$$

It is not difficult to calculate $\{\beta_{d,i}\}_{i=1}^{M}$ numerically, e.g., with QR decomposition. For a unsteady target flow, $\mathbf{X}_d(t)$ can be generated analogously with (36) for every $t \in [0, T]$.

The new cost functional is now derived as

$$J(\mathbf{X}(t), v(t)) = \int_0^T \frac{1}{2}(\mathbf{X}(t) - \mathbf{X}_d)^T \cdot \Psi \cdot (\mathbf{X}(t) - \mathbf{X}_d) + \frac{\sigma}{2}v^2(t)dt, \tag{37}$$

where

$$\left[\Psi\right]_{i,j} = \int_\Omega \langle \mathbf{\Phi}_i, \mathbf{\Phi}_j \rangle \, d\mathbf{x} \quad \text{for } i, j = 0, ..., M + 1. \tag{38}$$

The modified Dirichlet boundary control problem given in section 3 with the two state equations can be converted into the POD reduced order flow control problem, namely:

$$\min J(\mathbf{X}(t), v(t))$$

subject to: $\qquad\qquad\qquad\qquad\qquad\qquad (P_M)$

$$\mathbf{X}'(t) = \mathbf{F}(\mathbf{X}) + v(t)B\,,$$
$$\mathbf{X}(0) = \mathbf{X}_0\,.$$

The set of admissible controls $\mathcal{U}_{ad}$ remains

$$\mathcal{U}_{ad} = \{v \in L^2(0,T) : v_a(t) \le v(t) \le v_b(t) \quad \text{a.e. on } (0,T)\}\,.$$

We devote to investigate the existence of the optimal solution for (P_M) as well as the assumptions, for a detailed representative standard sample refer to [17].

Definition 2. *The Sobolev space is defined as*

$$H^1(0,T)^{M+2} := \{\mathbf{X}(t) \in L^2(0,T)^{M+2} :\ \exists \mathbf{X}'(t) \in L^2(0,T)^{M+2}\}\,.$$

Remark 1. $H^1(0,T)$ is compactly embedded in $C(0,T)$. This proof can be found in [6, Satz 3.2.4].

Theorem 3. *Let $[0,T]$ be a fixed interval and $\sigma > 0$, the admissible control set $\mathcal{U}_{ad}$ be non-empty. Let f_0 be convex and continuous in v. Assume that all successful states on $[0,T]$ satisfy an apriori bound*

$$|\mathbf{X}(t; \mathbf{X}_0, v)| \le C \quad \text{for all } v \in \mathcal{U}_{ad}, \text{ almost everywhere on } [0,T]\,. \qquad (39)$$

Then the POD optimal control problem (P_M) has optimal solution $v^* \in \mathcal{U}_{ad}$ with associated state $\mathbf{X}^* \in H^1(0,T)^{M+2}$.

Proof. The non-empty set of admissible controls is bounded in $L^2(0,T)$. For every $v \in \mathcal{U}_{ad}$ and suitable $\mathbf{X}_0$, there exists a unique solution of the state equation. Since J is bounded from below, $J(\mathbf{X}(t), v(t)) \ge 0$ and J has an infimum

$$0 \le j := \inf J(\mathbf{X}, v) \le \infty\,.$$

There is a minimizing sequence $(\mathbf{X}_n, v_n)$ of admissible pairs such that

$$J(\mathbf{X}_n, v_n) \to j \quad \text{as } n \to \infty\,.$$

Since the set of admissible controls $\mathcal{U}_{ad}$ is bounded, and all states with respect to the admissible controls are bounded, i.e., the apriori bound (39) (see apriori estimates in [10, Theorem 4.2, Theorem 4.7, Theorem 5.1, Theorem 5.2]), there exists a subsequence

$$(\mathbf{X}_{n_k}, v_{n_k}) \rightharpoonup (\mathbf{X}^*, v^*) \in H^1(0,T)^{M+2} \times L^2(0,T)\,. \qquad (40)$$

$\mathcal{U}_{ad}$ is convex and closed in $L^2(0,T)$. It follows that $\mathcal{U}_{ad}$ is weakly sequence closed and consequently $v^* \in \mathcal{U}_{ad}$. It remains to prove that the state limit $\mathbf{X}^*$ is the solution of the state equation with respect to v^*. Since

$$\mathbf{X}_{n_k} \rightharpoonup \mathbf{X}^* \in H^1(0,T)^{M+2}$$

and $H^1(0,T)$ is compactly embedded in $C(0,T)$, there exists a subsequence $\{\mathbf{X}_{n_{k_l}}\}_{l=1}^{\infty}$ of the subsequence $\{\mathbf{X}_{n_k}\}_{k=1}^{\infty}$ such that as $l \to \infty$

$$\mathbf{X}_{n_{k_l}} \to \mathbf{X}^* \text{ in } C(0,T)^{M+2} \text{ and } \mathbf{X}'_{n_{k_l}} \rightharpoonup (\mathbf{X}^*)' \text{ in } L^2(0,T)^{M+2}. \qquad (41)$$

Since $\mathbf{F}$ is continuous in $\mathbf{X}$ and $\mathbf{X}_{n_{k_l}} \to \mathbf{X}^*$ in $C(0,T)^{M+2}$, it follows as $l \to \infty$

$$\mathbf{F}(\mathbf{X}_{n_{k_l}}) \to \mathbf{F}(\mathbf{X}^*) \text{ in } C(0,T)^{M+2}.$$

It is known that $C(0,T)^{M+2} \hookrightarrow L^2(0,T)^{M+2}$, then

$$\mathbf{F}(\mathbf{X}_{n_{k_l}}) \rightharpoonup \mathbf{F}(\mathbf{X}^*) \text{ in } L^2(0,T)^{M+2}. \qquad (42)$$

Without loss of generality, we substitute the circumstantial index $_{n_{k_l}}$ with $_n$ such that

$$(\mathbf{X}_n, v_n) \rightharpoonup (\mathbf{X}^*, v^*) \in H^1(0,T)^{M+2} \times L^2(0,T), \quad \text{as } n \to \infty. \qquad (43)$$

Summarizing (40), (41) and (42) in the state equation of (P_M) and combining the notation of (43) yields

$$\underbrace{\mathbf{X}'_n}_{\rightharpoonup (\mathbf{X}^*)' \text{ in } L^2(0,T)^{M+2}} = \underbrace{\mathbf{F}(\mathbf{X}_n)}_{\rightharpoonup \mathbf{F}(\mathbf{X}^*) \text{ in } L^2(0,T)^{M+2}} + \underbrace{Bv_n}_{\rightharpoonup Bv^* \text{ in } L^2(0,T)^{M+2}}.$$

Note that $B \in \mathbb{R}^{M+2}$ is a constant vector with respect to the POD basis system $\{\mathbf{\Phi}_i\}_{i=1}^M$. Then as $n \to \infty$, we obtain that

$$(\mathbf{X}^*)' = \mathbf{F}(\mathbf{X}^*) + Bv^* \quad \text{in } L^2(0,T)^{M+2}.$$

That is to say, the state limit $\mathbf{X}^*$ in $L^2(0,T)^{M+2}$ is the solution of the state equation with respect to the optimal control v^* with an initial condition $\mathbf{X}_0$.

It is also known that f_0 is convex and continuous in v, then J is weakly lower-semicontinuous (see [5, Theorem 1.1]) and

$$j = \lim_{k\to\infty} \inf J(\mathbf{X}_{n_k}, v_{n_k}) \geq J(\mathbf{X}^*, v^*).$$

Since j is the infimum, i.e., $j \not> J(\mathbf{X}^*, v^*)$, it follows that $j = J(\mathbf{X}^*, v^*)$.

Next we need the first order necessary condition that enables us to distinguish the optimal control from the other controls in the set of admissible controls $\mathcal{U}_{ad}$. We remark that the formal Lagrangian technique can be employed again for the first order optimality condition, however the Pontryagin maximum principle is well-known as a standard result, which was proved by L.S. Pontryagin in 1956 and can be applied for the task.

We define the Hamiltonian by

$$H := p_0 f_0 + \sum_{i=1}^{M+2} p_i f_i.$$

The integrand of the (P_M) cost functional (37) is accordingly notated due to convenience as follows

$$f_{0,1} := \frac{1}{2}(\mathbf{X}(t) - \mathbf{X}_d)^T \cdot \Psi \cdot (\mathbf{X}(t) - \mathbf{X}_d), \quad f_{0,2} := \frac{\sigma}{2}v^2(t), \quad f_0 := f_{0,1} + f_{0,2}.$$

The right hand side of the (P_M) state equation, i.e., $\mathbf{F}(\mathbf{X}) + v(t)B$ can be rewritten as the scalar fields $\{f_i\}_{i=1}^{M+2}$ respectively. In general $p_0 = -1$, and we derive the adjoint equation,

$$\dot{p}_0 = -\frac{\partial H}{\partial \mathbf{X}_0} = 0,$$

$$\dot{p}_i = -\frac{\partial H}{\partial \mathbf{X}_i} = \frac{\partial f_{0,1}}{\partial \mathbf{X}_i} - \sum_{j=1}^{M+2} p_j \frac{\partial f_j}{\partial \mathbf{X}_i}, \quad \text{for } i = 1, ..., M+2.$$

Note that the transversality condition becomes

$$(p_1(T), ..., p_{M+2}(T))^T = \mathbf{0},$$

if the state $\mathbf{X}(t)$ at $t = T$ is completely unspecified. The adjoint equation can be composed in vectorial notation style and due to numerical execution of the backward system set $-w(t) = p(t)$

$$(AD) \quad \begin{cases} -\dot{w} &= [f_{0,1}]_{\mathbf{X}} + [\mathbf{F}]_{\mathbf{X}}^T w, \\ w(T) &= \mathbf{0}. \end{cases}$$

Let v^* be optimal, it is necessary that H attains its maximum at v^* for almost every $t \in [0, T]$.

$$\sup_{v \in \mathcal{U}_{ad}} H(\mathbf{X}, v, p) \Leftrightarrow \sup_{v \in \mathcal{U}_{ad}} \left(-\frac{\sigma}{2} v^2(t) + B^T p \cdot v(t) \right)$$

$$= \sup_{v \in \mathcal{U}_{ad}} \left(-\frac{\sigma}{2} v^2(t) - B^T w \cdot v(t) \right)$$

$$= \min_{v \in \mathcal{U}_{ad}} \left(\frac{\sigma}{2} v^2(t) + B^T w \cdot v(t) \right), \quad \text{if } \sigma > 0.$$

It is known that v^* solves the above minimizing problems, i.e., $v^* \in L^2(0, T)$ solves the following optimization problem for $\sigma > 0$

$$\min_{v \in \mathcal{U}_{ad}} \int_0^T \left(\frac{\sigma}{2} v^2(t) + v(t) B^T w \right) dt.$$

Then the variation inequality holds for $\sigma > 0$:

$$\int_0^T (\sigma v^* + B^T w)(v - v^*) dt \geq 0 \qquad \forall \, v \in \mathcal{U}_{ad}.$$

Summarizing the optimality system for the POD boundary control problem (P_M) yields

$$\text{state equation} \Rightarrow \begin{cases} \dot{\mathbf{X}}(t) = \mathbf{F}(\mathbf{X}) + v(t) B \\ \mathbf{X}(t_0) = \mathbf{X}_0 \end{cases}$$

$$\text{adjoint equation} \Rightarrow \begin{cases} -\dot{w} = \Psi \cdot (\mathbf{X}(t) - \mathbf{X}_d) + [\mathbf{F}]_{\mathbf{X}}^T \cdot w \\ w(T) = \mathbf{0} \end{cases}$$

$$\text{variation inequality} \Rightarrow \begin{cases} \int_0^T (\sigma v^* + B^T w)(v - v^*) dt \geq 0 \qquad \forall \, v \in \mathcal{U}_{ad}, \end{cases}$$

Briefly we give here the algorithm, which provides the optimal Dirichlet boundary for the Navier-Stokes equations equivalently by solving the above optimal control system.

Algorithm 2

1. Solve the Navier-Stokes equation (1) at n different time steps for the snapshots $\{\mathbf{u}_j\}_{j=1}^n$ with $z(t)$ and the associated steady flow $\mathbf{u}_0$ as initial condition.

2. Use **Algorithm 1** to calculate the M POD Basis.
3. Define $\mathbf{\Phi}_0 = \mathbf{u}_m(\mathbf{x})$ and $\mathbf{\Phi}_{M+1}(\mathbf{x}) = \mathbf{u}_z(\mathbf{x})$, which are given in (27) and (31).
4. Project the Navier-Stokes equation onto POD subspace and construct
   a) the correlative POD basis matrix Ψ as (38),
   b) $\tilde{B} = -\left[\Psi\right]_{i,M+1}$, for $i = 1, ..., M$,
   c) the stiffness matrix A of POD projection system,
   d) the nonlinearity matrix P_i, for $i = 1, ..., M$ and
   e) the initial condition $\mathbf{X}_0$.
5. Capture $\mathbf{X}_d$ or $\mathbf{X}_d(t)$ by (36) with QR decomposition.
6. Execute an optimization algorithm
   a) initialize $k := 0$ and $v^{(0)} = z'(t)$ for $t \in [0, T]$
   b) solve the POD state equation forward for $\mathbf{X}(t)$ with respect to $v^{(k)}$
   c) solve the adjoint equation backward for $w(t)$ with respect to $\mathbf{X}(t)$
   d) set the search direction, e.g., anti-gradient direction

$$dk = -(\sigma v^{(k)} + B^T \cdot w)$$

   e) determine sn with Armijo step size control
   f) $v^{(k+1)} = v^{(k)} + sn \times dk$
   g) $r = \|v^{(k+1)} - v^{(k)}\|$
   h) repeat (a)-(h) and set $k = k+1$, if r is not sufficient small. Otherwise stop the optimization, $v^* = v^{(k+1)}$
7. Solve $z'(t) = v^{(k+1)}$ and $z(0) = z_0$ for $z^*(t)$ as the optimal controlled boundary condition in (1),
8. Calculate the Navier-Stokes equations (1) with respect to the optimal Dirichlet boundary condition $z^*(t)$ to yield the optimal fluid flow.

5 Computational Result

To illustrate the result of the POD approach in solving the Dirichlet boundary flow control problem, several numerical examples are carried out in the same geometry. First of all, the geometry in which the numerical tests are to be calculated is a rectangle $\Omega \subseteq \mathbb{R}^2$ containing as in Figure 1 the inflow boundary Γ_i, outflow boundary Γ_o and wall $\Gamma \backslash (\Gamma_i \cup \Gamma_o)$.

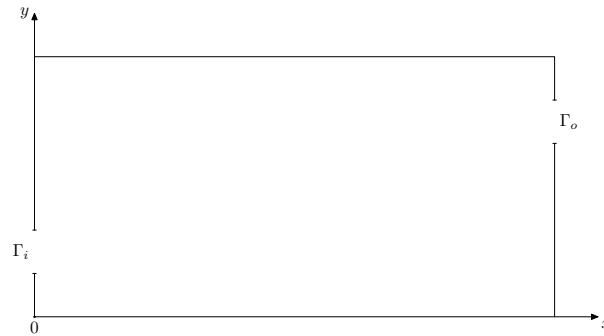The Navier-Stokes system (1) is solved in the time interval $[1, 10]$ for

FIG. 1: Domain Ω with inflow boundary Γ_i and outflow boundary Γ_{out}

generating snapshots ensemble. The sinusoidal function as one choice of the spatially dependent velocity field on inflow boundary is given

$$\mathbf{g}(\mathbf{x}) = \begin{pmatrix} \sin(\frac{y-y_0}{y_1-y_0}\pi) \\ 0 \end{pmatrix} \text{ and } \mathbf{x} = \begin{pmatrix} x \\ y \end{pmatrix}.$$

The linear profile $z(t) = z_0 t$ for $t \in [1, 10]$ is taken to complete the boundary setting. Two hundreds snapshots are recorded at $Re = 10000$ with equivalent time distance $\Delta t = \frac{T-1}{200-1}$.

The entries of correlative matrix C can be computed by trapezoidal integration schema. Its eigenvalue range in logarithmic scale is shown in Figure 2, which is solved by using matlab routine `eig`. As shown the eigenvalues drop quickly and thus very few models are able to carry the essential dynamic energy of the snapshots.
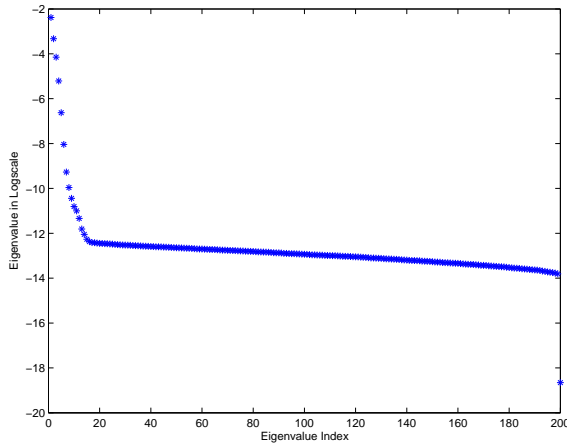
FIG. 2: Eigenvalues of the correlative matrix C

Table 1 displays percentage of the full order models energy captured by the POD reduced order models, e.g., 99.9999 percent of the full order models energy captured by only six basis functions. These six POD basis are chosen to represent the modified ensemble for carrying out the further numerical flow simulation and control experiments.

M	1	2	3	4	5	6
Energy in %	97.9758	99.7095	99.9452	99.9956	99.9998	99.9999
l^1 *Error*	0.005370	0.005305	0.005305	0.005305	0.005300	0.005300

Table 1: Percentage of full order model energy and l^1-norm difference between full order and POD reduced order models captured with $M = 1, ..., 6$

To complete the flow simulation with the POD basis, one should recast solution of the Navier-Stokes equations with the POD ansatz (26), where the coefficient function $\{\beta_i(t)\}_{i=1}^M$ are gained by decoupling (35) with Crank-Nicolson and 4th order Runge-Kutta schema. We compare the profiles of the flow computed with full order models and the POD reduced order models in Figure 3, which is recorded at $t = 9$ for various cross-sections of the spatial domain. Both simulations show quantitatively satisfactory agreement.
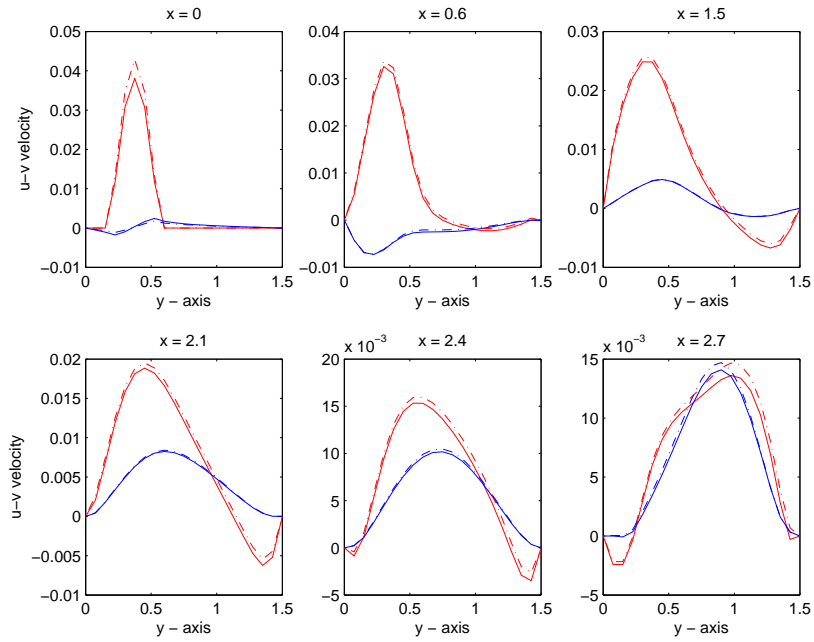
FIG. 3: Profile comparison of full order model(solid line) and POD reduced order models solution(dash-dot line); velocities u(red) and v(blue) at $t = 9$.

Before we start Galerkin POD control stage, the streamlines of the eight POD basis are shown in Figure 4 and Figure 5. $\boldsymbol{\Phi}_0$ displays the averaged flow, and the other POD basis are barely identified with any ordinary steady flow except for the last two POD basis $\boldsymbol{\Phi}_6$ and $\boldsymbol{\Phi}_7$. However, we remark they are quantitatively different, though they show very similar in streamline. Therefore, we compare the $\boldsymbol{\Phi}_6$ to $\boldsymbol{\Phi}_{1-5}$ and to $\boldsymbol{\Phi}_7$ respectively in horizonal velocity through various cross section in Figure 6 and Figure 7.
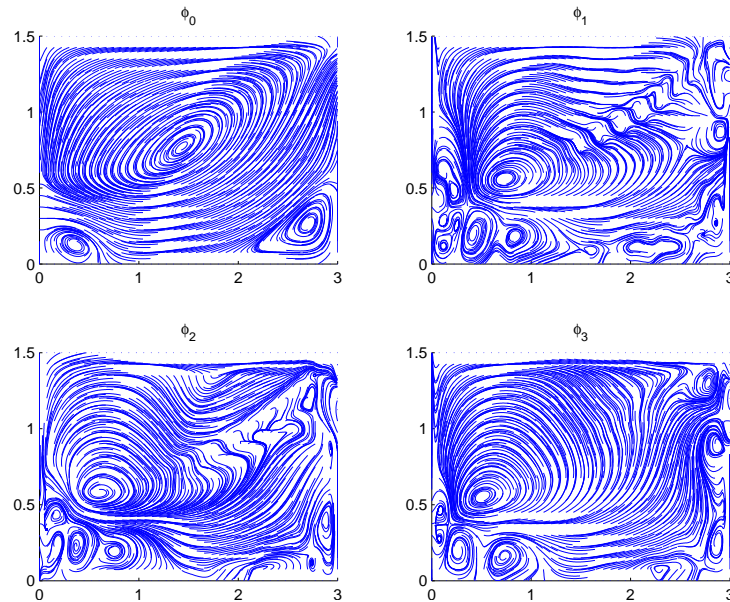
FIG. 4: The POD basis $\boldsymbol{\Phi}_0(x, y), \boldsymbol{\Phi}_1(x, y), \boldsymbol{\Phi}_2(x, y), \boldsymbol{\Phi}_3(x, y)$
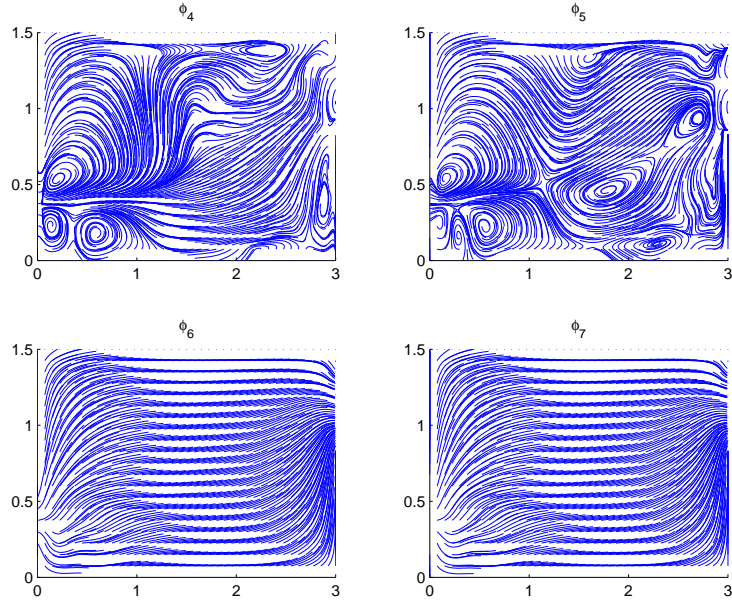
FIG. 5: The POD basis $\mathbf{\Phi}_4(x,y), \mathbf{\Phi}_5(x,y), \mathbf{\Phi}_6(x,y), \mathbf{\Phi}_7(x,y)$
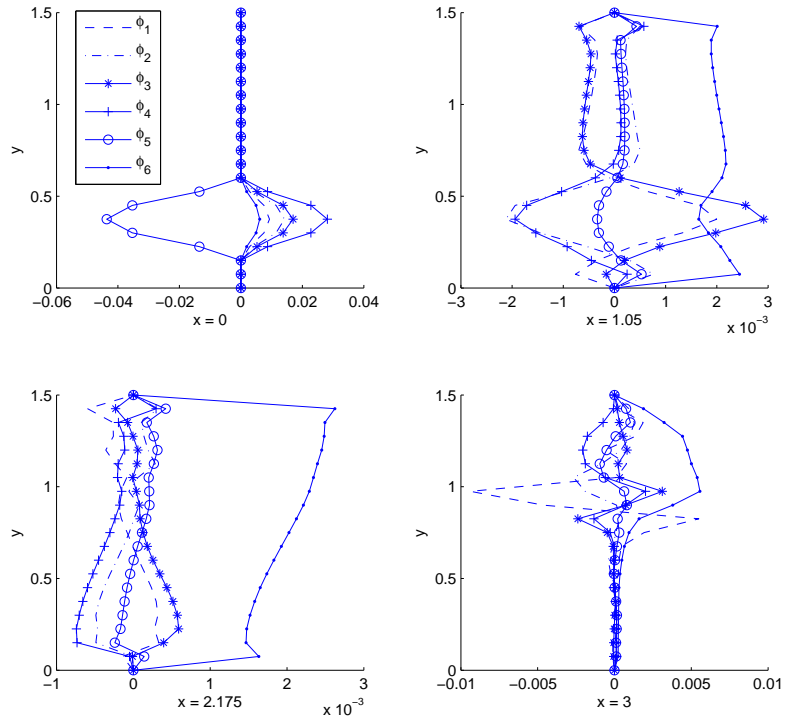
FIG. 6: The profile comparison between $\mathbf{\Phi}_6$ and $\mathbf{\Phi}_1 - \mathbf{\Phi}_5$
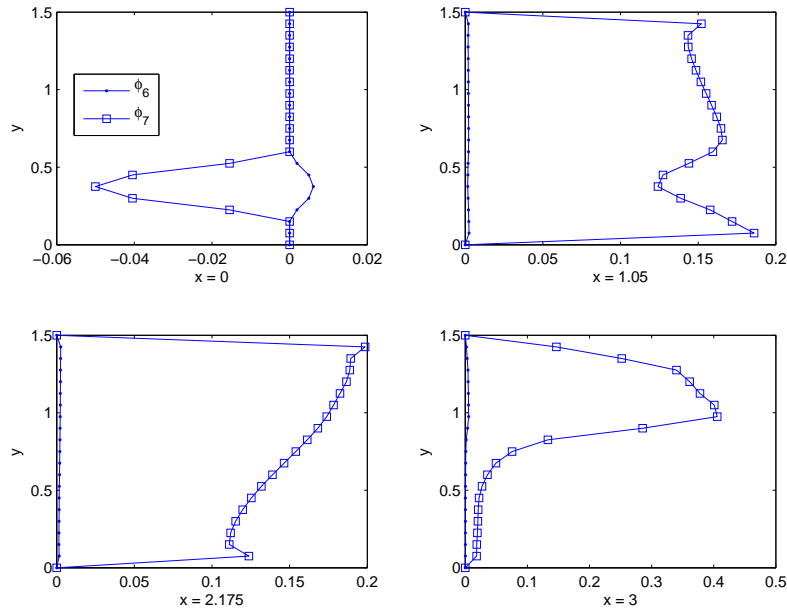
FIG. 7: The profile comparison between $\mathbf{\Phi}_6$ and $\mathbf{\Phi}_7$

5.1 Control Test I

It remains to allocate the expected flow samples to appraise the control quality with the Galerkin POD method. As the first test we set a steady flow U_d shown in Figure 8, which can be capture by solving steady Navier-Stokes equations with the inflow boundary $\mathbf{u}(\mathbf{x})\big|_{\Gamma_i} = z_d\,\mathbf{g}(\mathbf{x}) = 0.025\,\mathbf{g}(\mathbf{x})$ and the other boundary conditions prescribed by (1).

A start guess control $v^{(0)}$ is next required for the optimization. We start
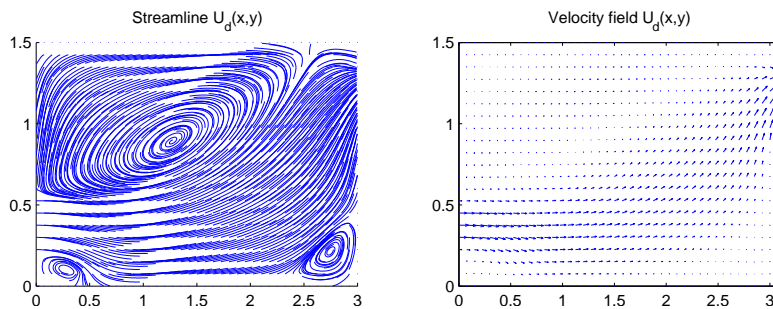
FIG. 8: The steady target flow with $z_d = 0.025$.

to control with $v^{(0)}(t) = z'(t) \equiv z_0$ for $t \in [1, 10]$, which is well-related to the current POD basis with respect to the snapshots ensemble generated by the inflow boundary condition $z(t) = z_0 t$ in $[1, 10]$.

In Figure 9, the optimal control $v^*(t)$ in POD system and the corresponding $z^*(t)$ are displayed at different σ values. The parameter σ is found to regularize the effort in the controller design. Figure 9 presents the relatively smaller value of σ could achieve the expected flow more quickly due to the light weighted control-effort term $v^2(t)$ in the cost functional J.
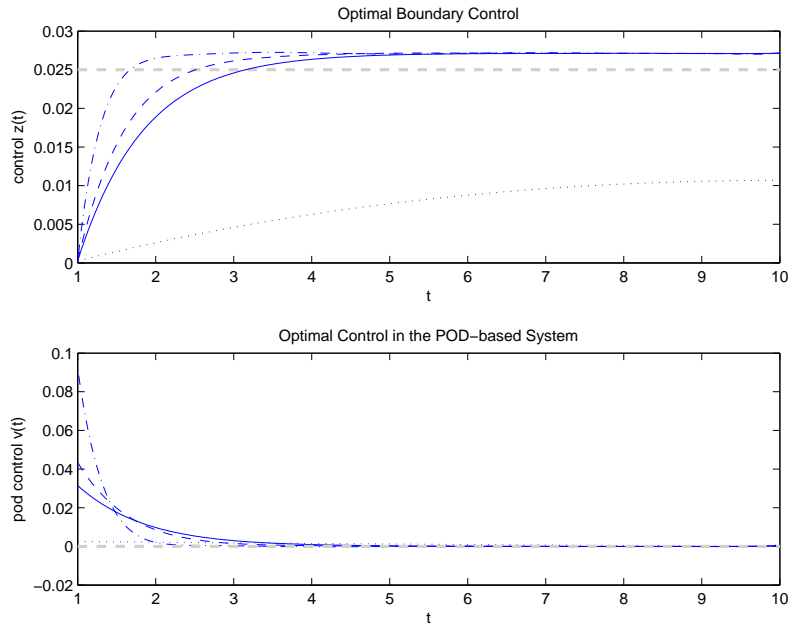
FIG. 9: Optimal controls of the Navier-Stokes equations and POD-based system for different values of σ: 10(dotted line), 1/10(solid line), 1/20(dashed line), 1/100(dash-dot line) and expected boundary profile (grey dashed line) respectively.

At different σ values the integrands $f_0(X^*(t), v^*(t))$ in the cost functional are evaluated with respect to the by CG method solved optimal controls v^* and the associated states X^*. Figure 10 presents straightforwardly the optimal steady flow is reached rapidly as σ is set to be 0.05 or smaller.
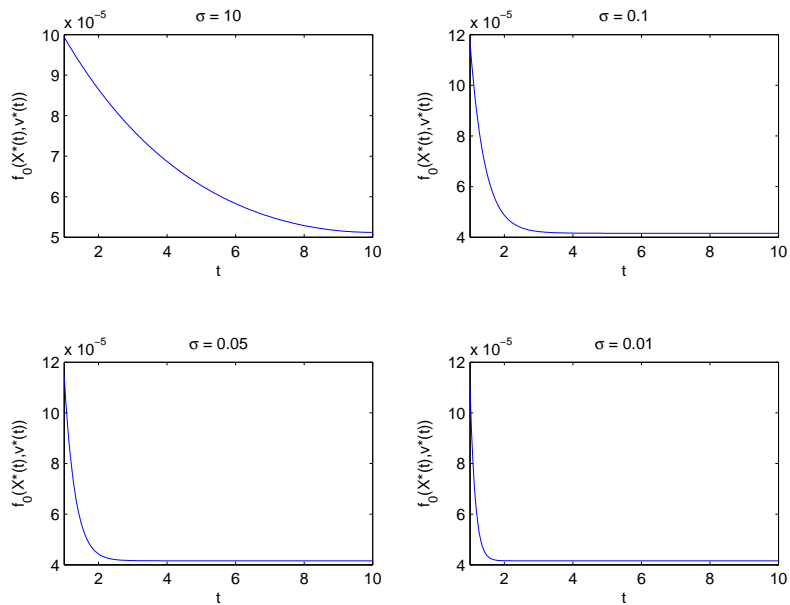
FIG. 10: The evaluated integrand $f_0(X^*(t), v^*(t))$ for $t \in [1, 10]$ at different σ

For a clear sight of the POD captured boundary control effect, Figures 11-12 demonstrate streamlines of the snapshots as uncontrolled flow and the POD controlled flow, from which we confirm that the POD controlled flow had no vortex in the left upper corner during all time steps. We refer reader to note that streamline of the expected steady flow in Figure 8 exhibits also no vortex there, which is set in the objective function as the pattern flow and should be imitated by controlling with the optimal Dirichlet boundary condition z^*. Finally, Figure 12 at $t = 10$ shows a good effect of the POD boundary control, meanwhile an extra vortex has grown up there in the uncontrolled flow.
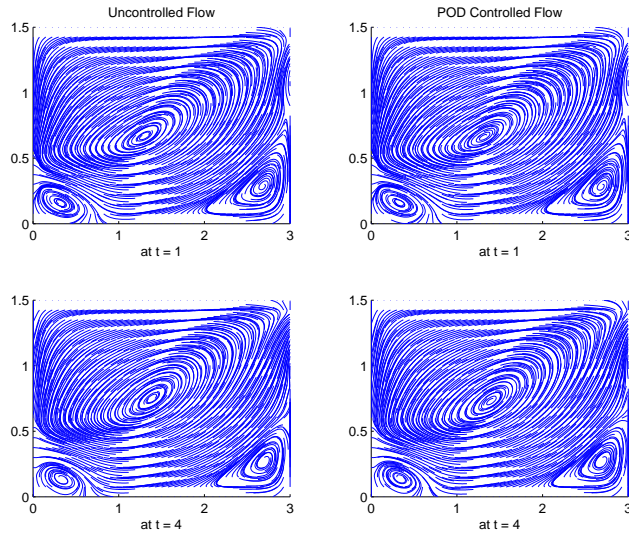

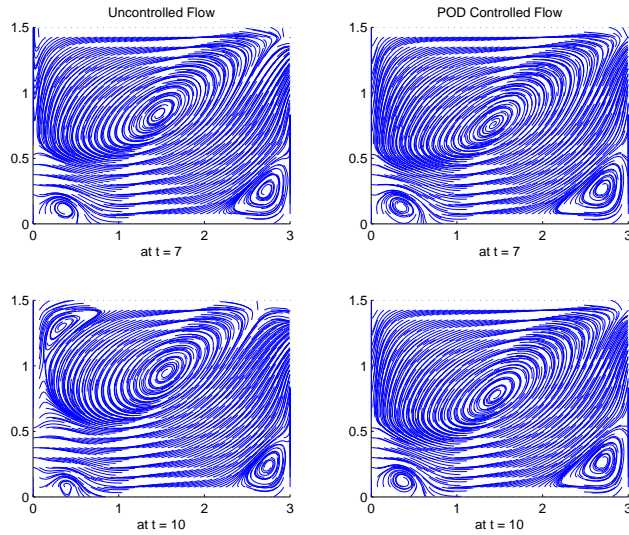FIG. 11: POD Controlled and uncontrolled flow streamlines comparison at $t = 1$ and $t = 4$.

FIG. 12: POD Controlled and uncontrolled flow streamlines comparison at $t = 7$ and $t = 10$.

5.2 Control Test II

In the unsteady flow matching case we could devise an analytical design parameter $z_d(t)$ in $[0, 10]$ and capture the unsteady target flow pattern $U_d(\mathbf{x}, t)$ by solving (1) with $z_d(t)$ on the inflow Σ_i. By utilizing the eight POD basis system, the second control test can be performed, in which the unsteady target flow $U_d(\mathbf{x}, t)$ described above is set in the cost functional.

Firstly we give the inflow boundary condition on Σ_i, for $t \in [0, 10]$

$$U_d(\mathbf{x}, t)\Big|_{\Sigma_i} := z_d(t)\mathbf{g}(\mathbf{x}) = \Big[\frac{1}{10}\Big(1 - t\Big)^2\Big(1 - \cos\big(\frac{5}{6 + 5t}\big)\Big) + \frac{86}{5000}\Big]\mathbf{g}(\mathbf{x})$$

where $\mathbf{g}(\mathbf{x})$ remain unchanged. Analogously as (36) for every $t \in [0, 10]$, $\mathbf{X}_d(t)$ can be figured out with $z_d(t)$.

The optimization with the Galerkin POD induces the optimal solutions for the second control example as in Figure 13, which shows excellent agreement between the POD optimal solution at $\sigma = 0.001$ and analytical target. Note that these optimal solutions are solved with the known initial condition of target flow, i.e., steady flow with inflow $z_d(0)\mathbf{g}(\mathbf{x})$. However it is not always self-evident to possess the same initial condition as the target flow $U_d(0, \mathbf{x})$. Next we explore control flexibility of Galerkin POD approach without being revealed the initial condition of target flow. From Figure 14 we can confirm the optimal control with a different initial condition succeeds. All POD controlled $z^*(t)$ regarding σ start with $z^*(0) = z_0$ at $t = 0$, which is originally for generating snapshots. Obviously the optimal trajectories $z^*(t)$ for almost everywhere in $[0, 10]$ accommodates the target $z_d(t)$.

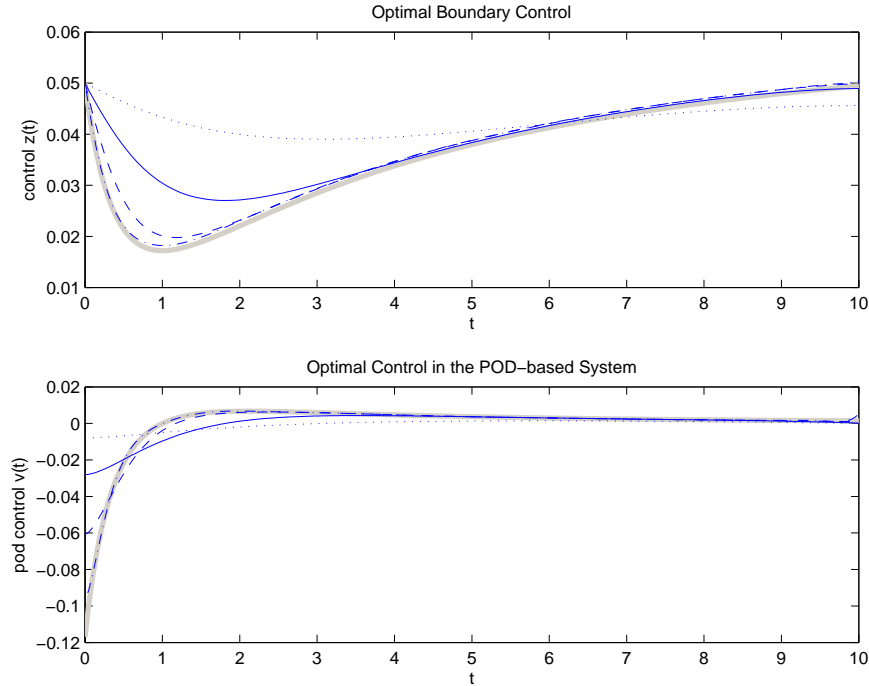In both numerical experiments, eight POD basis functions calculated

FIG. 13: POD optimal solutions for different values of σ: 1(dotted line), 1/10(solid line), 1/100(dashed line), 1/1000(dash-dot line) compared with analytical function $z_d(t)$(grey thick solid line) and its derivative $v_d(t) = z'_d(t)$ (grey thick solid line).
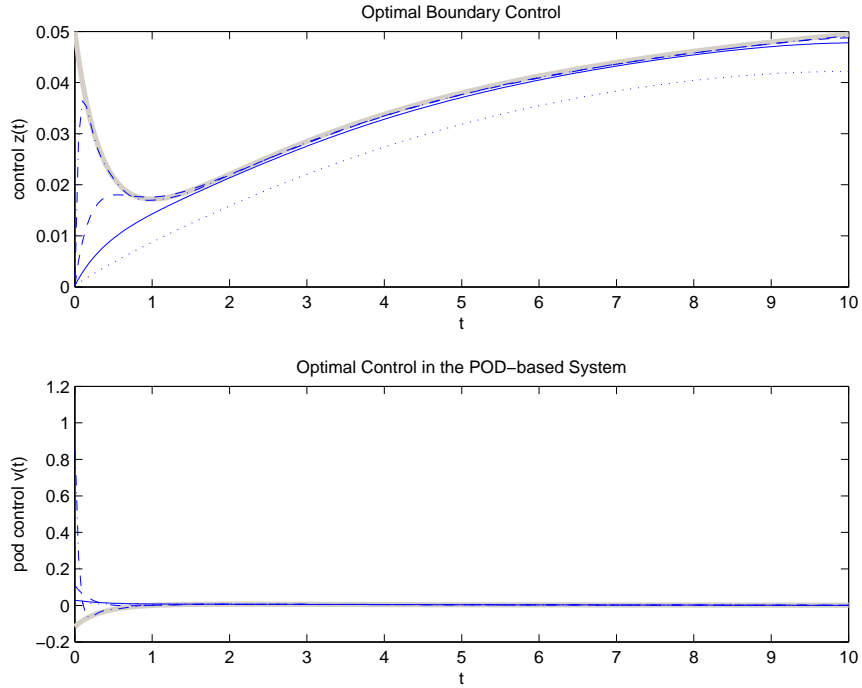
FIG. 14: POD optimal solutions for different values of σ: 1(dotted line), 1/10(solid line), 1/100(dashed line), 1/1000(dash-dot line) compared with analytical function $z_d(t)$(grey thick solid line) and its derivative $v_d(t) = z'_d(t)$ (grey thick solid line).

with respect to the snapshot ensemble have been used for the optimization (see. Algorithm II). All control candidates $v(t) \in L^2(0,T)$ are not certainly well related to these eight POD basis functions during the optimization. However, these POD basis functions enable us to capture the optimal control $v^* \in L^2(0,T)$. If the POD basis functions and control candidates $v(t) \in L^2(0,T)$ are not well related to each other, i.e., the POD basis functions can not simulate the behavior of the current $v(t)$ related flow, then the so-called adaptive POD control should be applied, on which the standard work [14] is for boundary control problems and [1] for the distributed control problems.

5.3 Control Test III

For the third control example, we attempt to replace the original snapshots ensemble, which is generated by linear function $z(t)$ on the inflow boundary. Setting another inflow profile, for instance $z_d(t)$ used as target inflow condition in the second control test, namely

$$z(t) = \frac{1}{10}(1-t)^2\Big(1 - \cos\big(\frac{5}{6+5t}\big)\Big) + \frac{86}{5000}\,,$$

yields the new snapshots ensemble.

As usual we make firstly the POD ansatz, in which $\mathbf{u}_z$ can be constructed by following (31). However, in this case one may capture

$$\mathbf{u}_z(\mathbf{x}) = \frac{\mathbf{u}_{z_1} - \mathbf{u}_{z_0}}{z_1 - z_0} = \frac{\mathbf{u}_{z_1} - \mathbf{u}_{z_0}}{\underbrace{z(10) - z(0)}_{\approx 0}}\,. \tag{44}$$

This singularity can be removed by dividing $z(t)$ with respect to t into different parts according to its monotone. For $t \in [0, 1]$, $z(t)$ is monotonously decreasing and for $t \in [1, 10]$ monotonously increasing. Each monotonous part of $z(t)$ is suitable for generating $\mathbf{u}_z$, and we choose the latter

$$\mathbf{u}_z(\mathbf{x}) = \frac{\mathbf{u}_{z(10)} - \mathbf{u}_{z(1)}}{z(10) - z(1)} \,.$$

A new target flow $U_d(\mathbf{x}, t)$ should subject to the following analytical inflow boundary condition

$$U_d(\mathbf{x}, t)\Big|_{\Sigma_i} = \Big[\Big(\frac{1}{10}\big(1 - \cos(\frac{5}{5t+6})\big)(1-t)^2 + \frac{1}{100}\Big)\cos(\frac{t+5}{10}) + \frac{3}{250}\Big]\mathbf{g}(\mathbf{x}) \,.$$

The technique given above does not ruin the result, see Figure 15. As mentioned the last POD basis can be built successfully for the purpose of optimal control, if one gains the snapshots ensemble established by such a nonlinear inflow time profile.
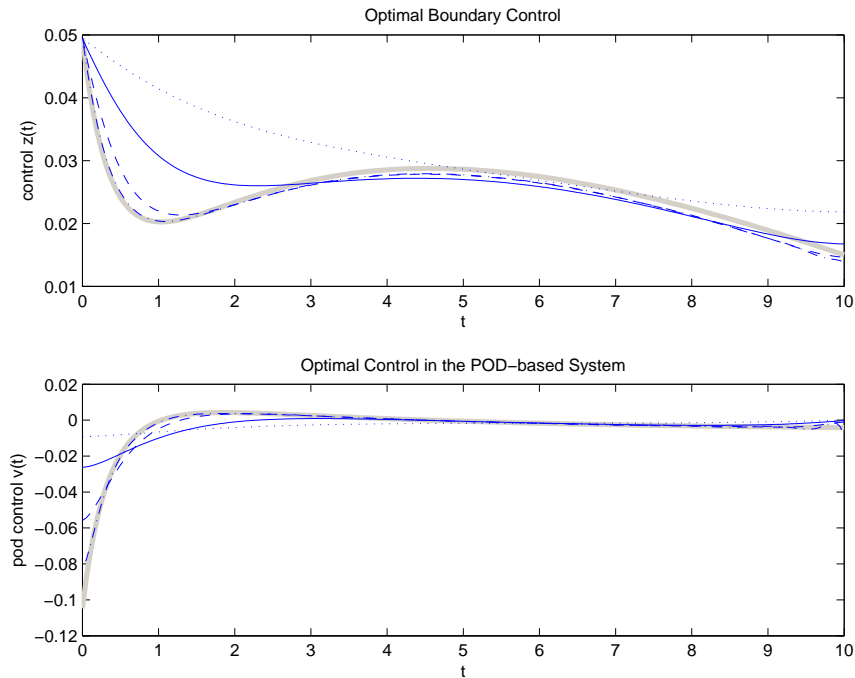

FIG. 15: POD optimal solutions for different values of σ: 1(dotted line), 1/10(solid line), 1/100(dashed line), 1/1000(dash-dot line) compared with analytical configuration (grey thick solid line).

References

1. K. Afanasiev, M. Hinze. Adaptive control of a wake flow using proper orthogonal decomposition. *Lecture Notes in Pure and Applied Mathematics: Shape Optimization and Optimal Design, Marcel Dekker.* 216, 317-332, 2001.
2. M. Berggren. Numerical solution of a flow-control problem: Vorticity reduction by dynamic boundary action. *SIAM J. Sci. Comput.,* Vol 19, No.3, pp. 829-860, 1998.

3. E. Casas, M. Mateos, F. Tröltzsch. Error Estimates for the Numerical Approximation of Boundary Semilinear Elliptic Control Problems. *Computational Optimization and Applications,* 31: 193-219, 2005.

4. E. Casas and J. P. Raymond. Error Estimates for the Numerical Approximation of Dirichlet Boundary Control for Semilinear Elliptic Equations. *SIAM J. Control Optim.* Vol. 45, No. 5, pp. 1586-1611, 2006.

5. B. Dacorogna. *Weak Continuity and Weak Lower Semicontinuity of Non-Linear Functionals. Lecture Notes in Mathematics 922.* Springer-Verlag Berlin Heidelberg NewYork, 1982.

6. E. Emmrich. *Gewöhnliche und Operator-Differentialgleichungen.* Vieweg, 2004.

7. M. D. Gunzburger and S. Manservisi. The velocity tracking problem for Navier-Stokes flows with boundary control. *SIAM. J. Control Optim.*, 39: No. 2, pp. 594-634, 2000.

8. M. Hinze and K. Kunisch. Second order methods for boundary control of the instationary Navier-Stokes system. *ZAMM*, 84: 171-187, 2004.

9. L. S. Hou and S. Ravindran. A penalized Neumann control approach for solving an optimal Dirichlet control problem for the Navier-Stokes equations. *SIAM J. Control Optimization*, 36: 1795-1814, 1998.

10. K. Kunisch and S. Volkwein. Galerkin proper orthogonal decomposition methods for a general equation in fluid dynamics. *SIAM J. Numer. Anal.*, 40: 492-515, 2002.

11. Lumley JL. The structure of inhomogeneous turbulence. *Atm. Turb. and Radio Wave Prop. (Yaglom and Tatarsky eds.) Nauka, Moscow,* pp 166-178, 1967

12. E. R. Pinch. *Optimal control and the Calculus of Variations.* Oxford University Press, 1993.

13. S. Ravindran. A reduced order approach to optimal control of fluids using proper orthogonal decomposition. *Int. J. Numer. Methods Fluids*, 34(5): 425-448, 2000.

14. S. S. Ravindran. Reduced-Order Adaptive Controllers for Fluid Flows Using POD. *J. Sci. Comput.*, 15(4): 457-478, 2000.

15. R.L. Sani and P.M. Gresho. Resume and remarks on the open boundary condition mini-symposium. *International Joundal of Numerical Methods in Fluids.* 18: 983-1008, 1994.

16. F. Tröltzsch and D. Wachsmuth. Second-order sufficient optimality conditions for the optimal control of instationary Navier-Stokes equations. *PAMM · Proc. Appl. Math. Mech. 4*, 628-629, 2004

17. F. Tröltzsch. *Optimale Steuerung partieller Differentialgleichungen.* Vieweg, Berlin, 2005.

18. F. Tröltzsch and S. Volkwein. POD a-posterior error estimates for linear-quadratic optimal control problems. *Accepted by Computational Optimization and Applications*, DOI 10.1007/s110589-008-9224-3.

19. S. Volkwein. Proper orthogonal decomposition and singular value decomposition. *SFB-Preprint No. 153,* 1999.

20. S. Volkwein. Optimal Control of a Phase-Field Model Using Proper Orthogonal Decomposition. *ZAMM. Z. Angew. Math. Mech.*, 81(2): 83-97, 2001.

21. Y. Wang. Reduced order optimal control for Fluid Flow by Using Galerkin POD. Master Thesis, 2008.